Scaling and exact solutions for the flux creep problem in a slab superconductor

D. V. Shantsev,[1,2] Y. M. Galperin,[1,2] and T. H. Johansen[1,*]
[1]*Department of Physics, University of Oslo, P. O. Box 1048, Blindern, 0316 Oslo, Norway*
[2]*A. F. Ioffe Physico-Technical Institute, Polytekhnicheskaya 26, St. Petersburg 194021, Russia*
(Received 3 August 2001; published 25 April 2002)

The flux creep problem for a superconductor slab placed in a constant or time-dependent magnetic field is considered. Logarithmic dependence of the activation energy on the current density is assumed, $U=U_0\ln(J/J_c)$, with a field dependent J_c. The density B of the magnetic flux penetrating into the superconductor is shown to obey a scaling law, i.e., the profiles $B(x)$ at different times t can be scaled to a function of a single variable x/t^{β}. We found exact solution for the scaling function in some specific cases, and an approximate solution for a general case. The scaling also holds for a slab carrying transport current I resulting in a voltage $V\propto I^p$, where $p\sim 1$. When the flux fronts moving from two sides of the slab collapse at the center, the scaling is broken and $V(I)$ crosses over to $V\propto I^{U_0/kT}$.

DOI: 10.1103/PhysRevB.65.184512 PACS number(s): 74.60.Ge, 74.25.Ha

I. INTRODUCTION

Thermally activated hopping of flux lines between pinning sites, or flux creep, controls both the magnetic and transport properties of superconductors under various external conditions. In particular, it is responsible for the frequently observed fast magnetic relaxation and the highly nonlinear local voltage-current curves. Flux creep is specifically pronounced in high-temperature superconductors because there the pinning energies are small, while the operation temperatures are high.[1,2]

In the majority of theoretical and experimental studies of flux creep[2–5] a superconductor is first placed in an increasing or decreasing field, thus acquiring a nonzero magnetization, M. The field is then kept constant and the relaxation of M with time is examined. In the present work we address a different problem—flux penetration into a nonmagnetized superconductor, $M(t=0)=0$. After turning on a constant or time-dependent magnetic field, a flux front propagates from the surface with some time-dependent velocity. In the case of a long slab in parallel field two planar flux fronts propagate from each side. Absence of a characteristic spatial scale suggests a possibility for scaling solutions, i.e., the flux density profile $B(x)$ at different times t is a function of a single variable x/t^{β}, where β is a constant. Indeed, such scaling was demonstrated in Ref. 6 for an instantaneous turn-on of a constant applied field, and assuming a superconductor characterized by a logarithmic dependence of the pinning energy on the current density.

In this work we have sought for the whole class of flux creep problems having solutions with a single-parameter scaling. This class turned out to be a lot broader than considered in Ref. 6, insofar as it extends to situations with time-dependent applied fields, $B_a(t)\propto t^{\alpha}$, and a general field-dependent critical current density $J_c(B)$. We also report scaling solutions for the flux creep in a superconductor carrying a transport current. There the flux creep manifests itself in a number of experimental observations like a relaxation in the resistance, and that the voltage across the sample depends on the current sweep rate, etc.[7–11]

The paper is organized as follows. In Sec. II the basic equations are formulated. Section III brings out the scaling properties of their solution. In Sec. IV two cases allowing an exact analytical solution are considered. The subsequent sections report the implications of our results for measurable quantities: B, J, and E distributions, magnetization, and voltage. Finally, the main conclusions are summarized.

II. FORMULATION OF THE PROBLEM

Consider a semi-infinite superconductor (filling the half-space $x>0$) placed in an external magnetic field $B_a(t)$ directed along the z axis (see Fig. 1). The position- and time-dependent flux density (or magnetic induction) and shielding current in the sample are denoted as $B(x,t)$ and $J(x,t)$, respectively. Both **J** and the electric field **E** are directed along the y axis.

From the Ampere and Faraday laws one then has

$$\mu_0 J=-\partial B/\partial x, \tag{1}$$

$$\partial B/\partial t=-\partial E/\partial x. \tag{2}$$

To describe the superconductor we assume that $E=vB$, where $v=v_0\exp(-U/kT)$ is the velocity of the thermally activated vortex motion over the barrier U. With a logarithmic dependence $U(J)=U_0\ln(J_c/J)$ it follows that

$$E(J,B)=v_0|B|\,|J/J_c|^n\operatorname{sgn} J, \tag{3}$$

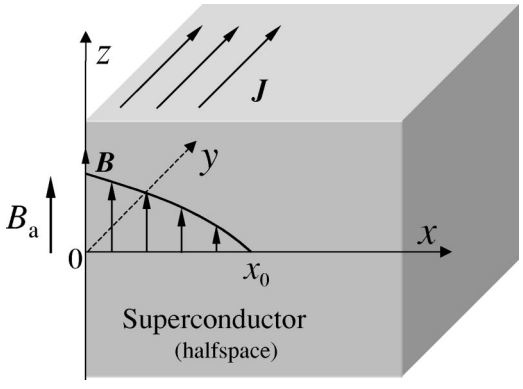


FIG. 1. Superconductor slab in an applied magnetic field.

 ©2002 The American Physical Society

where the exponent $n=U_0/k_BT$ depends on the temperature T. The critical current density J_c usually depends on $|B|$, and in the bulk part of the paper it will be assumed that this is described by[12]

$$J_c(B)=J_{c0}|B_0/B|^{\gamma}. \tag{4}$$

To avoid parameters with inconvenient dimensions we introduced here two constants, J_{c0} and B_0, a characteristic current density and induction, in addition to the exponent γ.[13] With $\gamma=0$ one has a constant J_c (the Bean model), while for $\gamma=-1/n$ one has an $E-J$ relation,

$$E=v_0B_0|J/J_{c0}|^n\mathrm{sgn}\,J, \tag{5}$$

which is B-independent. Such an $E(J)$ has been used by many authors since it allows a significant simplification of the analysis. It is justified when the magnetic field inside the superconductor is essentially uniform, in particular, when a small perturbation $\delta B(x,t)$ is added to a superconductor cooled in a large dc field.

The electrodynamic problem defined by Eqs. (1)–(4) can be reformulated as a nonlinear diffusion equation for the flux density,

$$\frac{\partial B}{\partial t}=\frac{v_0}{(\mu_0J_{c0}B_0^{\gamma})^n}\frac{\partial}{\partial x}\left(|B|^{1+\gamma n}\left|\frac{\partial B}{\partial x}\right|^{n-1}\frac{\partial B}{\partial x}\right). \tag{6}$$

Similar equations can be written also for J and E.

We will first consider a totally flux free superconductor which at $t\geqslant 0$ experiences an increasing applied magnetic field given by

$$B_a(t)=B_0(t/\tau)^{\alpha},\quad \alpha>0, \tag{7}$$

where τ is another constant. For $\alpha=0$ and $\alpha=1$ this describes an instant field step and a linear ramping up, respectively. By introducing the dimensionless variables

$$b=\frac{B}{B_0},\ \tilde{x}=x\frac{\mu_0J_{c0}}{B_0},\ \tilde{t}=\frac{t}{\tau},\ j=\frac{J}{J_{c0}},\ \epsilon=\frac{E}{v_0B_0}, \tag{8}$$

and removing the redundant parameter definition by choosing

$$B_0=\mu_0J_{c0}v_0\tau, \tag{9}$$

the Eq. (6) acquires the form[14]

$$\frac{\partial b}{\partial\tilde{t}}=\frac{\partial}{\partial\tilde{x}}\left(|b|^{1+\gamma n}\left|\frac{\partial b}{\partial\tilde{x}}\right|^{n-1}\frac{\partial b}{\partial\tilde{x}}\right). \tag{10}$$

The boundary condition becomes

$$b(0,\tilde{t})=\tilde{t}^{\alpha}, \tag{11}$$

at the superconductor surface.

III. SCALING

The flux creep problem Eqs. (10) and (11) is solved by writing the flux density in the scaling form

$$b(\tilde{x},\tilde{t})=\tilde{t}^{\alpha}f(\xi),\quad \xi=\tilde{x}\tilde{t}^{-\beta}, \tag{12}$$

with

$$\beta=\frac{1+\alpha n(1+\gamma)}{1+n}. \tag{13}$$

By substitution one finds that the scaling function $f(\xi)$ satisfies the differential equation

$$-\alpha f+\beta\xi f'=(f^{1+\gamma n}|f'|^n)', \tag{14}$$

where it was used that $f\geqslant 0$, and $f'\leqslant 0$, i.e., the flux density decreases monotonously as one moves away from the surface. The boundary conditions become

$$f(0)=1,\quad f(\xi_0)=0, \tag{15}$$

where the last one arises from the physical requirement that the scaling function vanishes at the flux front, which is located at $\xi=\xi_0$. From Eq. (12) it follows immediately that the flux front advances with time according to

$$\tilde{x}_0(\tilde{t})=\xi_0\tilde{t}^{\beta}. \tag{16}$$

For the case $\alpha=0$ (constant applied field) one has $\beta=1/(n+1)$, while a larger α increases the exponent β.

Using Eqs. (1) and (3) one finds that also the current density and electric field have scaling properties, namely

$$\begin{aligned} j(\tilde{x},\tilde{t})&=\tilde{t}^{\alpha-\beta}|f'(\xi)|,\\ \epsilon(\tilde{x},\tilde{t})&=\tilde{t}^{\alpha+\beta-1}f_{\epsilon}(\xi),\quad f_{\epsilon}\equiv|f'|^nf^{1+\gamma n}. \end{aligned} \tag{17}$$

The scaling behavior of the ac losses is found from a similar analysis of the product $j(\tilde{x},\tilde{t})\epsilon(\tilde{x},\tilde{t})$.

When the magnetic field is instantly turned on and then kept constant ($\alpha=0$), exact scaling relations are obtained even when the power-law Eq. (4) is relaxed and replaced by *any* $J_c(B)$. Considering here

$$J_c(B)=\frac{J_{c0}}{s(B/B_0)}, \tag{18}$$

where s is a general function, a diffusion equation for the flux density similar to Eq. (10) can be derived, giving

$$\frac{\partial b}{\partial\tilde{t}}=\frac{\partial}{\partial\tilde{x}}\left[|b|s^n(b)\left|\frac{\partial b}{\partial\tilde{x}}\right|^{n-1}\frac{\partial b}{\partial\tilde{x}}\right], \tag{19}$$

where the same dimensionless variables Eqs. (8) and (9) are used. The scaling form of the flux density [Eq. (12)] is still applicable where now $b(\tilde{x},\tilde{t})=f(\tilde{x}\tilde{t}^{-1/(n+1)})$. The equation for the scaling function $f(\xi)$ is changed to

$$\xi f'/(n+1)=[fs^n(f)|f'|^n]' \tag{20}$$

while the boundary conditions (15) are the same. The flux front, current density, and electric field are now given by

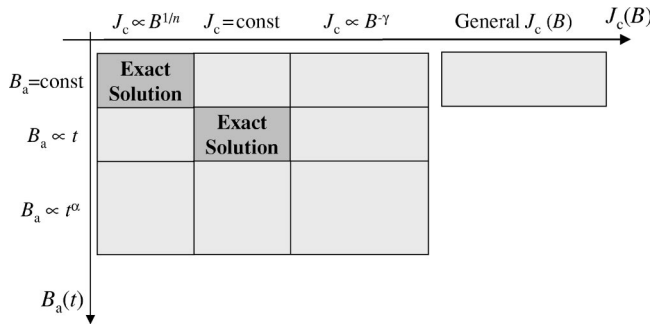


FIG. 2. Summary of our results. The diagram illustrates where the flux creep problem has scaling solutions. A full analytical solution is found for two particular cases.

$$\tilde{x}_0 = \xi_0 \tilde{t}^{1/(n+1)},$$

$$j(\tilde{x},\tilde{t}) = \tilde{t}^{-1/(n+1)} |f'(\xi)|,$$

$$\epsilon(\tilde{x},\tilde{t}) = \tilde{t}^{-n/(n+1)} f_\epsilon(\xi), \quad f_\epsilon \equiv |f'|^n f s^n(f), \tag{21}$$

and hence, they also possess scaling properties in this case.

As we have formulated the flux creep problem, the wide variety of possible situations is represented by the set of three independent parameters, n, γ, and α. For a given parameter set the scaling function $f(\xi)$ can be obtained by solving the Eqs. (14) and (20) numerically. Interestingly, one may in two special cases find exact analytical solutions, as shown in the next section. Shown in Fig. 2 is a summary of our findings regarding scaling solutions for the flux creep problem in various situations. From this $J_c(B)$-$B_a(t)$ diagram it is seen that scaling holds for a majority of conceivable conditions. Note that even if the scaling function itself is unknown one may test predicted scaling behaviors experimentally, e.g., by analyzing flux density profiles $B(x,t)$ measured at different times. Plotting $B(x,t)/B_a(t)$ versus $x/x_0(t)$ is expected to result in a collapse into a scaling function $f(\xi)$. Other practical consequences of the scaling concerning the magnetization and voltage behavior are discussed below.

IV. EXACT SOLUTION FOR PARTICULAR CASES

A. Constant field, *B*-independent *E*(*J*)

The solution for this case will be worked out in considerable detail in order to illustrate some basic features of the scaling properties of the physical quantities. Suppose that at $t=0$ a constant applied magnetic field, B_0, is turned on, i.e., one has $\alpha=0$. Furthermore, let $\gamma=-1/n$, which leads to the commonly assumed current-voltage law, Eq. (5). From Eqs. (12) and (13) the scaling law has then the form

$$b(\tilde{x},\tilde{t}) = f(\xi), \quad \xi = x\,\tilde{t}^{-1/(n+1)}, \tag{22}$$

and Eq. (14) for the scaling function reduces to

$$[\xi - n(n+1)|f'|^{n-2} f'']f' = 0. \tag{23}$$

This equation has two real solutions for f' consistent with $\partial B/\partial x \leqslant 0$, namely,

$$-f' = \begin{cases} \left[\dfrac{n-1}{2n(n+1)}(\xi_0^2 - \xi^2)\right]^{1/(n-1)}, & \xi \leqslant \xi_0, \\ 0, & \xi \geqslant \xi_0. \end{cases} \tag{24}$$

The parameter ξ_0 is an integration constant that is determined from the following interpretation of Eq. (24). Noting that since $-f'(\xi)$ directly represents the spatial profile of the current $J(x,t)$, the solution with $f'=0$ is identified as the one valid for the Meissner-state region where also $b=0$. The point $\xi=\xi_0$, then defining the flux penetration front, is determined by $f(\xi_0)=0$ using the solution valid for the penetrated (mixed-state) region. We find

$$\xi_0 = \left[2n\frac{n+1}{n-1}F(1)^{1-n}\right]^{1/(n+1)}, \tag{25}$$

where the function F is defined as

$$F(z) = \int_0^z (1-y^2)^{1/(n-1)} dy. \tag{26}$$

The value $F(1)$ can be expressed through Γ functions as

$$F(1) = \frac{\sqrt{\pi}}{2}\Gamma\left(\frac{n}{n-1}\right) \Big/ \Gamma\left(\frac{3}{2} + \frac{1}{n-1}\right). \tag{27}$$

The result for the flux density profile becomes

$$b(\tilde{x},\tilde{t}) = 1 - \frac{F(\tilde{x}/\tilde{x}_0(\tilde{t}))}{F(1)}, \quad 0 \leqslant \tilde{x} \leqslant \tilde{x}_0, \tag{28}$$

where the position of the flux front, $\tilde{x}_0$, is moving with time according to

$$\tilde{x}_0(\tilde{t}) = \xi_0 \tilde{t}^{1/(n+1)}. \tag{29}$$

It then also follows that the normalized current density $j = -\partial b/\partial \tilde{x}$, and electric field in the flux penetrated region, $0 \leqslant \tilde{x} \leqslant \tilde{x}_0$, are given by

$$j(\tilde{x},\tilde{t}) = \frac{1}{F(1)}\frac{1}{\tilde{x}_0(\tilde{t})}\left[1 - \left(\frac{\tilde{x}}{\tilde{x}_0(\tilde{t})}\right)^2\right]^{1/(n-1)},$$

$$\epsilon(\tilde{x},\tilde{t}) = j(\tilde{x},\tilde{t})^n. \tag{30}$$

The differential resistivity $\partial E/\partial J \propto j^{n-1}$ therefore varies in space as a parabola having a maximum value at the edge.

Figure 3 shows the distribution of the magnetic induction, current density, and electric field for $n=3$ and 11. As the time increases, the flux penetrates deeper into the sample accompanied by a smaller slope of the flux density profile, i.e., a decay of current density. The electric field profile follows the behavior of $J(x)$, although decreasing much more rapidly due to the strongly nonlinear $E(J)$ law. As the power n increases the field and current distributions are seen to become more linear. In the limit $n=\infty$ one has $F(z)=z$ and $\xi_0=1$, and hence $\tilde{x}_0(\tilde{t})=1$. The temporal dependences then vanish, and the behavior reduces to $b=1-x/\delta$, $j=1$, and $\epsilon=0$ for $0 \leqslant x \leqslant \delta$, where $\delta = B_0/\mu_0 J_{c0}$. Thus, the well-known results of the Bean model are reproduced.

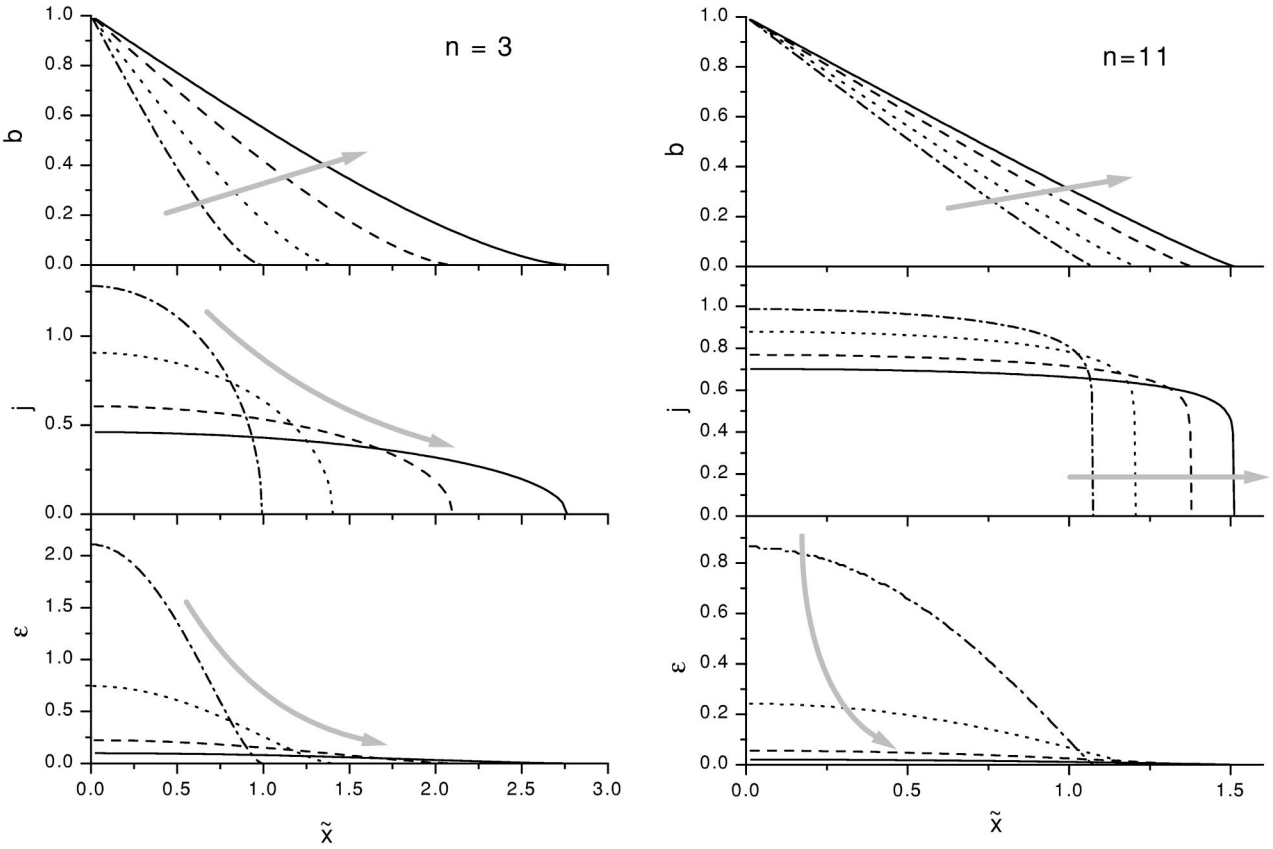


FIG. 3. Distributions of the normalized flux density, current density, and electric field after a sudden turn-on of a constant applied magnetic field. A B-independent $E(J)$, i.e., $\gamma=-1/n$, is assumed, and the plots are made for $n=3$ and 11. The arrows indicate time direction, and the curves correspond to $\tilde{t}=0.05$, 0.2, 1, and 3.

B. Linearly increasing field, constant J_c

For the linear sweep case, $B_a(t)=\dot{B}_a t$ ($\dot{B}_a=$const), and a constant J_c, i.e., $\alpha=1$ and $\gamma=0$, the flux creep problem has a surprisingly simple solution. It follows from Eq. (6) that

$$B(x,t)=\dot{B}_a t[1-x/x_0(t)], \quad x\leqslant x_0, \tag{31}$$

and the region $x>x_0$ is flux free. The flux front propagates linearly in time,

$$x_0(t)=\frac{\dot{B}_a}{\mu_0 J_c}\left(\frac{\mu_0 J_c v_0}{\dot{B}_a}\right)^{1/(n+1)} t. \tag{32}$$

Remarkably, this solution coincides with the Bean model behavior where in the penetrated region the flux profile is a straight line, and the current density is uniform,

$$J(x)=J_c(\dot{B}_a/\mu_0 J_c v_0)^{1/(n+1)}=\text{const}. \tag{33}$$

The electric field $E(x)$ becomes proportional to $B(x)$,

$$E(x,t)=v_0(\dot{B}_a/\mu_0 J_c v_0)^{n/(n+1)}B(x,t), \tag{34}$$

and hence, this quantity also is linear in both x and t. All these profiles are presented in Fig. 4(b). For larger field sweep rates, $\dot{B}_a$, the current density and electric field are higher, while the penetration depth at a given B_a is smaller.

The results of this subsection, unlike the results of the rest of the paper, can be used also to describe the flux distribution at large enough fields when the flux penetrates the whole slab. The current then flows in the opposite direction in the left and right halves of the slab, but with the same density as defined by Eq. (33). The magnetic field in the left half is given by a linear profile defined by Eq. (31), where x_0 is still given by Eq. (32), though it does not have the meaning of the flux front position anymore. In the right half $B(x)$ is a mirror image of that in the left half.

V. SUMMARY OF *B*, *J*, AND *E*

The evolution of the flux density, current density, and electric field distributions found numerically is presented in several graphs. Figure 4 shows results for the applied field linearly increasing in time, while Fig. 5, as well as Fig. 3, for an instant turn-on of a constant field. From these graphs the following conclusions can be drawn.

(i) The flux density profile is found convex for $\gamma\geqslant 0$, i.e., for constant J_c or J_c monotonically decreasing with B. It also means that $dJ/dx>0$, i.e., the current density increases as x approaches the flux front. For B-independent $E(J)$ the picture is the opposite; $|J|$ is maximum at the edge, and the $B(x)$ profile is concave; see Figs. 3 and 4(a). This behavior is expected for a field-cooled superconductor when a small ad-

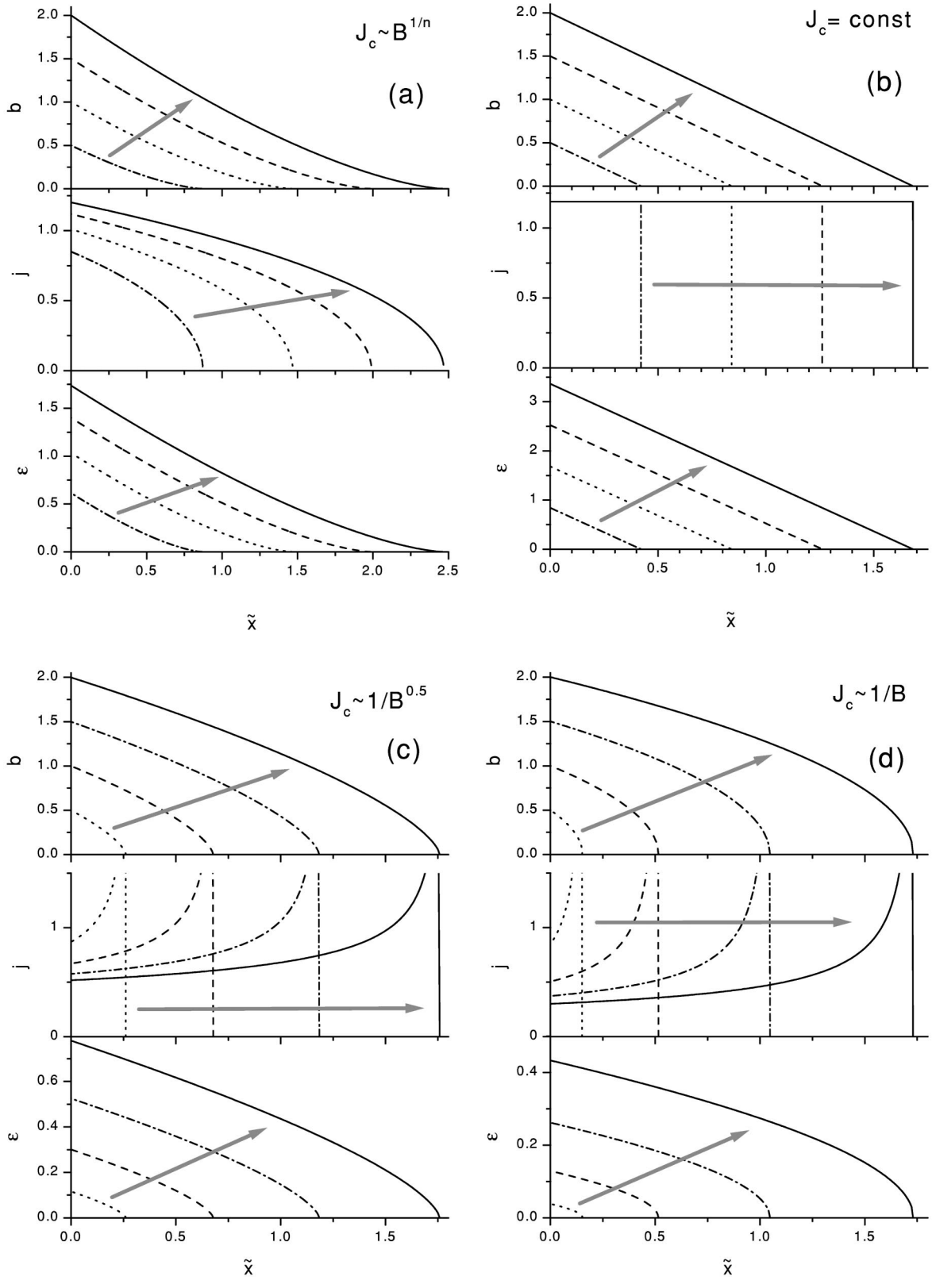


FIG. 4. Distributions of the normalized flux density, current density, and electric field at equidistant times, $\tilde{t}=0.5$, 1, 1.5, and 2. The applied field is *linearly increasing*, and $n=3$. (a)–(d) differ in $J_c(B)$ dependence: (a) B-independent $E(j)$, Eq. (5); (b) constant J_c ($J_c=2\dot{B}_a/\mu_0 v_0$), a case solved exactly in Sec. IV B; (c) and (d) J_c decreases with increase of $|B|$. The arrows indicate the time direction.

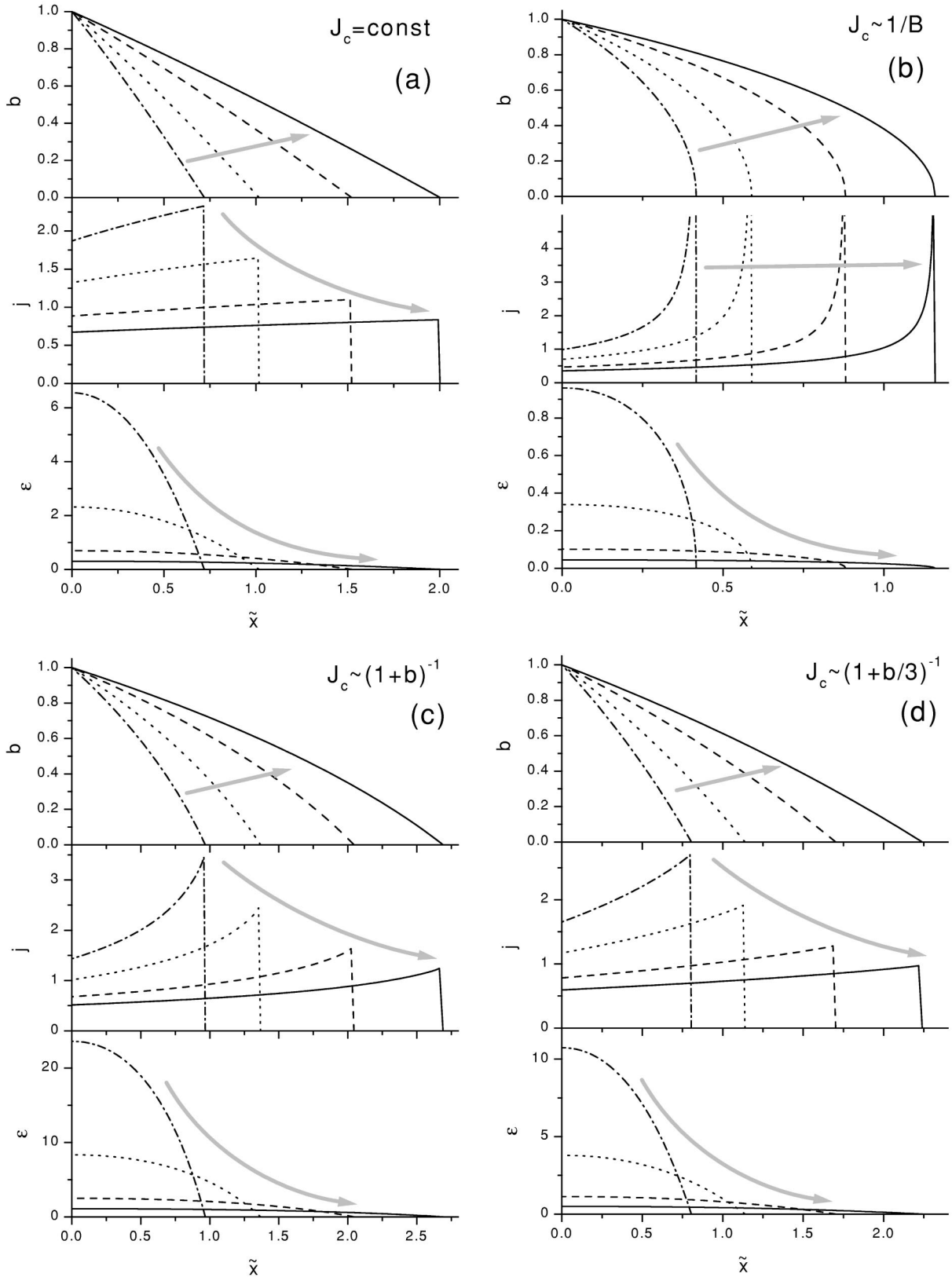
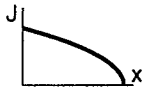
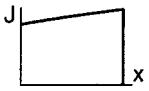
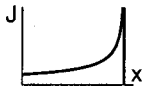
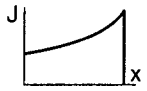
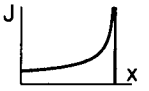


FIG. 5. Distributions of the normalized flux density, current density, and electric field at different times, $\tilde{t}=0.05$, 0.2, 1, and 3. The applied field is turned on at $\tilde{t}=0$ and kept *constant*, and $n=3$. (a)–(d) differ in $J_c(B)$ dependence: (a) constant J_c; (b) $J_c=J_{c0}/b$; (c,d) the Kim model, $J_c=J_{c0}/(1+b)$ and $J_c=J_{c0}/(1+b/3)$, respectively. The arrows indicate the time direction.

TABLE I. The shape of the current density profiles and the parameter ξ_0 characterizing the flux front dynamics, Eq. (16), in different regimes. The parameter a describes the approximate solution Eq. (44) for the scaling function f.

n	B-independent $E(j)$ ($\gamma=-1/n$)	$j_c=$ const ($\gamma=0$)	$j_c(B)\propto 1/B$ ($\gamma=1$)	The Kim model $J_c=J_{c0}(1+B/kB_0)^{-1}$
	Constant field, $B_a=B_0\Theta(t)$ $(\alpha=0)$			
	 see Fig. 3	 see Fig. 5(a)	 see Fig. 5(b)	 see Fig. 5(c,d)
3	exact solution, Eq. (28)	$\xi_0=1.521$, $a=0.105$	$\xi_0=0.881$, $a=0.032$	$\xi_0=2.044$, $a=0.42$ for k=1, n=3
7		$\xi_0=1.346$, $a=0.045$	$\xi_0=0.724$, $a=0.014$	
15		$\xi_0=1.212$, $a=0.021$	$\xi_0=0.628$, $a=0.007$	$\xi_0=1.702$, $a=0.25$ for k=3, n=3
33		$\xi_0=1.119$, $a=0.010$	$\xi_0=0.568$, $a=0.004$	
	Linear increase, $B_a=\dot{B}_a t$ $(\alpha=1)$			
	 see Fig. 4(a)	 see Fig. 4(b)	 see Fig. 5(d)	NO SCALING
3	$\xi_0=1.468$, $a=0.016$	exact solution, Eqs. (31-32)	$\xi_0=0.514$, $a=-0.004$	
7	$\xi_0=1.164$, $a=0$		$\xi_0=0.503$, $a=-0.002$	
15	$\xi_0=1.071$, $a=0$		$\xi_0=0.501$, $a=0.000$	
33	$\xi_0=1.031$, $a=0$		$\xi_0=0.499$, $a=0.001$	

ditional field is applied. When comparing these results to experimental data one should keep in mind that the shape of the observed $B(x)$ profile can easily be affected by demagnetization effects. However, the sign of dJ/dx for the current density profile seems to be robust, which is confirmed by the flux creep simulations for a thin film geometry.[15–18] Schematic $J(x)$ profiles for the most important cases are shown in Table I.

(ii) Even when B_a increases linearly with time, the flux penetration can proceed with acceleration or deceleration depending on the $J_c(B)$ dependence. This is illustrated in Fig. 4 where the panels (a)–(d) are ordered according to the $J_c(B)$ behavior, and the time intervals between the curves are equal. Only in (b) is the flux front moving with a constant velocity. In (a) the speed is slowing down, while in (c) and (d) it is increasing. In the latter case, ramping of the applied field leads to an effective reduction of J_c, and hence to larger electric fields and faster penetration. (a), (b), and (c,d) correspond to $\beta<1$, $\beta=1$, and $\beta>1$, respectively, where the exponent β given by Eq. (13) controls the growth of the flux penetrated region, Eq. (16).

(iii) The electric field has always a maximum at the edge and decreases monotonically with x, which follows from $\partial E/\partial x=-\dot{B}\leqslant 0$. Physically, this occurs simply because all the vortices enter the slab through the edge region where the flux motion is thus most intense. The second space derivative of E is proportional to $\partial J/\partial t$, and one can find different curvatures of the E-field profile for different cases.

VI. MAGNETIZATION

Since the nonlinear flux diffusion has a sharp front located a finite distance from the surface, the solution applies also to the case of a slab of *finite* width $2w$ provided w is larger than the penetration depth, x_0. The flux then penetrates the slab from both sides with nonoverlapping profiles.

The time-dependent magnetization of the slab is given by

$$-\mu_0 M=B_a-\frac{1}{w}\int_0^w B(x)dx, \tag{35}$$

where B is nonzero only in the region, $0<x<x_0(t)$. Substituting here the scaling law, Eq. (12), one obtains

$$-\mu_0 M(t)=B_a(t)\left[1-A\frac{x_0(t)}{w}\right], \quad 0\leqslant x_0\leqslant w, \tag{36}$$

where A is a number equal to the average value of the scaling function in the penetrated region:

$$A=\frac{1}{\xi_0}\int_0^{\xi_0} f(\xi)d\xi. \tag{37}$$

For the exact solution considered in Sec. IV A one finds $A=(n-1)/[2nF(1)]<1/2$. For the exact case in Sec. IV B where the B profile is linear, one has $A=1/2$. For flux density profiles with a convex shape, which are found when J_c decreases with B, one has $A>1/2$.

Expressing the time dependence explicitly, the magnetization can be written as

$$-\mu_0 M(\tilde{t})=B_a(\tilde{t})[1-A(\tilde{t}/\tilde{t}^*)^\beta], \quad 0\leqslant\tilde{t}\leqslant\tilde{t}^*, \tag{38}$$

where $\tilde{t}^*$ is the time it takes for the flux to completely penetrate the slab, i.e., $\tilde{t}^*=(\tilde{w}/\xi_0)^\beta$. For the fully penetrated state, $\tilde{t}>\tilde{t}^*$, the time dependence of M is essentially different, and one expects a kink in the magnetization relaxation rate, as first predicted in Ref. 6

VII. TRANSPORT CURRENT AND NONSTATIONARY $V(I)$

Most results found in the paper are also relevant to a superconductor carrying a transport current. The flux penetration into a slab biased with transport current is governed by the same equations as those for a slab placed in an applied magnetic field. The difference is that for the transport current case the current flows in the same direction on both edges of the slab. However, this is not important as long as the two penetrating flux fronts do not meet in the slab center. The boundary condition $B(x=0)=B_a$ for the applied field case should be replaced now by $B(x=0)=\mu_0 I/2$, where I is the transport current per unit height of the slab.

It is interesting to analyze the voltage V measured on the superconductor carrying a transport current I. It is obvious that V is not a unique function of I but also strongly depends on how I changes with time. In a conventional experimental setup the voltage contacts are attached to the superconductor surface; thus the measured voltage is determined by the electric field in the surface layer only, $V(t)=E(x=0,t)L$, where L is the distance along y between the contacts.

The electric field at the edge has a power dependence on time given by Eq. (17), since $f_\epsilon(0)$ is just a number. Thus, from Eq. (13) one obtains the following power-law voltage-current relation,

$$V\propto I^p, \quad p=1+\frac{n}{n+1}\left(1-\frac{1}{\alpha}+\gamma\right). \tag{39}$$

Note that the exponent p of the integral $V(I)$ can be much different from the exponent n characterizing the local $E(j)$. Actually, p is only weakly sensitive to n, especially for large n. Moreover, *increase* in n can sometimes lead to a *decrease* in p.

For large transport currents when the flux penetrates the whole sample the present analysis is not valid. Then the current density will be distributed over the slab more or less uniformly, and one can expect that the integral voltage-current curve will reflect the local one, i.e., $V\propto J^{n+1}$. The crossover between low-current and high-current parts in $V(I)$ has been reproduced by numerical simulations in Ref. 8. This crossover should be accessible experimentally since the exponent p for an incomplete flux penetration is of the order of unity, while the exponent n for the full penetration is temperature dependent and can be very large.

The exponent α in Eq. (39) defines the time dependence of the transport current, $I(t)\propto t^\alpha$. For larger α $V(I)$ becomes steeper until the exponent p saturates. For $\alpha=0$, i.e., when the current is turned on and kept constant, the voltage decays with time. This voltage relaxation has been earlier observed experimentally[9–11] and reproduced by numerical simulations.[9,11] It is accompanied by relaxation of current distribution, as illustrated by Fig. 5. According to Eq. (17), the voltage decay is described by $V\propto t^{-n/(n+1)}$, in particular $V\propto 1/t$ at low temperatures when n is large.

Remarkably, for small enough α the voltage will *decrease* with *increasing* current. For example, for $\alpha=1/3$ and $\gamma=0$, one obtains

$$V\propto I^{-(n-1)/(n+1)}, \tag{40}$$

in particular, $V\propto 1/I$ at low temperatures. Physically, a decrease of voltage is related to the same relaxation process which takes place for any external conditions. Increase of I with time supplies more current to the superconductor and tends to increase the voltage. If I increases slow enough, then the first process is dominant, and the measured $V(I)$ curve should give voltage decreasing as the current increases. The evolution of flux, current, and electric field distributions for this interesting case is shown in Fig. 6.

For the experimentally most relevant case of a linearly increasing current, $I=\dot{I}\,t$ (i.e., $\alpha=1$), one obtains from Eqs. (17) and (8)

$$V=\frac{\mu_0 v_0 L|f'(0)|^n}{2}\left(\frac{\mu_0^\gamma \dot{I}}{2^{1+\gamma}v_0 J_{c0}B_0^\gamma}\right)^{n/(n+1)} I^{1+\gamma n/(n+1)}. \tag{41}$$

For a constant J_c, or $\gamma=0$, we come to the exactly solvable case considered in Sec. IV B, and the expression further simplifies to

$$V=\frac{\mu_0 v_0 L}{2}\left(\frac{\dot{I}}{2J_c v_0}\right)^{n/(n+1)} I. \tag{42}$$

In this case the superconductor behaves like an *Ohmic* conductor. Deviations from the Ohmic behavior can be caused by a B dependence of J_c. In particular, if J_c decreases with B, the exponent of the $V(I)$ curve becomes larger than unity [see Eq. (41)]. Meanwhile, at small I the superconductor always behaves Ohmically since the self-field is small and the $J_c(B)$ dependence can be ignored. These results are in agreement with numerical simulations reported in Ref. 7.[19]

We also note that when the transport current is ramped faster, the voltage at a given current is larger, $V\propto \dot{I}^{\,n/(n+1)}$. This observation is in agreement with results of numerical simulations and experiment on Bi-based tapes.[9]

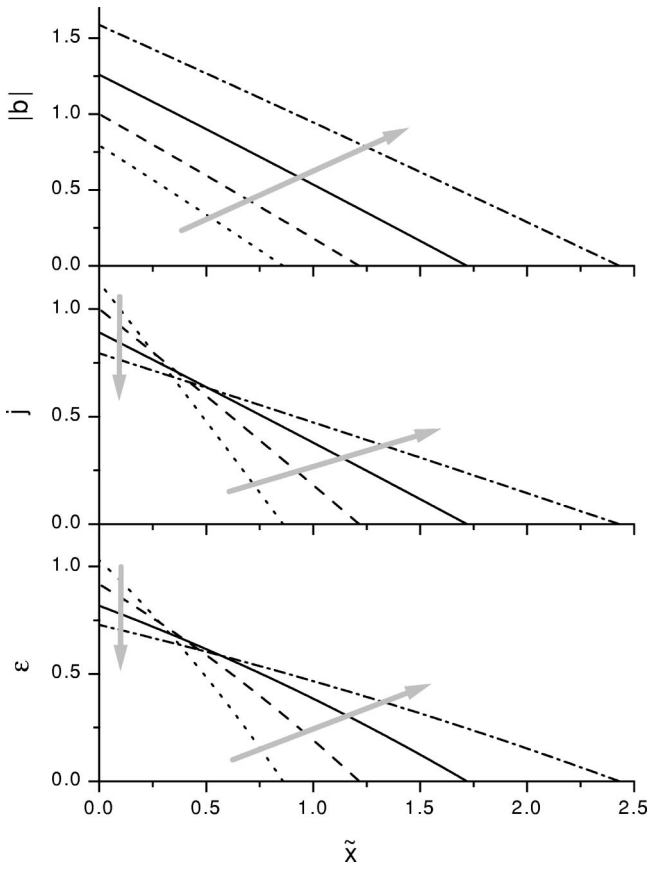


FIG. 6. Distributions of the normalized flux density, current density, and electric field at different times, $\tilde{t}=0.5$, 1, 2, and 4. The transport current increases with time as $I \propto t^{1/3}$, while $J_c=\text{const}$ and $n=3$. The voltage, which is proportional to $\epsilon(x=0)$, decreases with time, as shown by the arrows indicating the time direction.

VIII. APPROXIMATE SOLUTION

In a general case Eqs. (14) and (20) with boundary conditions (15) cannot be solved analytically. Near the flux front $f \to 0$, and Eq. (14) reduces to $(\text{const}+\beta\xi_0)^{1/n}=f^{\gamma}|f'|$. Therefore, the behavior of the scaling function f is determined only by the $J_c(B)$ law at small B, and

$$f(\xi) \propto (\xi_0-\xi)^{1/(1+\gamma)}, \quad \xi \to \xi_0. \tag{43}$$

This result holds true for any $J_c(B)$ which has asymptotic behavior $J_c \propto B^{-\gamma}$ at $B \to 0$, e.g., $\gamma=0$ for the Kim model.

Surprisingly, a very good approximate solution for f in the *whole* region $0 \leqslant \xi \leqslant \xi_0$ is given by the expression

$$f(\xi)=(1-\xi/\xi_0)^{1/(1+\gamma)}(1+a\xi). \tag{44}$$

Values of ξ_0 and a for several common dependences $J_c(B)$, including the Kim model, and values of n have been found numerically and listed in Table I. Expressions for ξ_0 and a in a general case can be found by substituting f from Eq. (44) into Eq. (14) and analyzing expansion in powers of $(\xi_0-\xi)$. Then, one obtains

$$\frac{1}{a}=\frac{2n(1+p)(p+\alpha n)}{p^2(p-\alpha)}-1, \quad p=1/(1+\gamma), \tag{45}$$

$$\xi_0^{n+1}=\frac{n+1}{1+\alpha n(1+\gamma)}\,\frac{(1+a)^{n(1+\gamma)}}{(1+\gamma)^n}. \tag{46}$$

Since the scaling function $f(\xi)$ usually has a very simple shape, we find that the approximate expressions fit the exact solutions with a good accuracy, e.g., the deviation is less than 1% for all cases shown in Figs. 4 and 5.

IX. CONCLUSIONS

The propagation of magnetic flux into a slab superconductor has been considered using the flux creep approach with a logarithmic current dependence of the activation energy. The dynamic behavior was found to possess scaling for a general $J_c(B)$ when a constant magnetic field is suddenly applied to the superconductor, and for a power-law $J_c(B)$ in case of an applied field ramped up with a general power dependence on time. For two particular cases of the creep problem an exact analytical solution could be found.

The main results obtained in this work are as follows:

(1) The flux density profiles at different times follow the scaling law, $B(x,t)=B_a(t)f(xt^{-\beta})$. Similar scaling applies to the current density and electric field profiles.

(2) The flux density profile is convex for penetration into a zero-field-cooled slab, and concave for a slab cooled in a large field.

(3) At constant J_c and linearly increasing B_a the $B(x)$ and $J(x)$ profiles at any time coincide with the Bean-model profiles.

(4) The flux front position is a power function of time given by Eqs. (16) and (13). The front moves through the slab with an increasing or decreasing velocity depending on the material's $J_c(B)$.

(5) The explicit time dependence of the magnetization is found.

(6) For a partially penetrated slab carrying a transport current I, the voltage V is a power of I, with an exponent different from that of the local $E(J)$ relation. A pronounced crossover in the $V(I)$ curve at the point of full penetration is predicted.

(7) For a small transport current increasing linearly with time, the Ohmic behavior $V \propto I$, is found.

(8) For a stationary transport current the voltage decays as $V \sim 1/t$.

(9) An increase of transport current can be accompanied by a decrease of voltage, in particular, $V \sim 1/I$ when $I \propto t^{1/3}$.

All the conclusions can be tested experimentally: (1)–(4) by spatially resolved techniques, and (5)–(9) by integral measurements. Our results presented by Eqs. (38) and (39) allow us to infer the material properties such as local $E(J)$ or $J_c(B)$ characteristics from integral measurements of magnetization and voltage.

ACKNOWLEDGMENTS

The financial support by the Research Council of Norway is gratefully acknowledged. We appreciate discussions with E. H. Brandt and V. M. Vinokur.

*Email address: t.h.johansen@fys.uio.no

[1] Y. Yeshurun and A.P. Malozemoff, Phys. Rev. Lett. **60**, 2202 (1988).
[2] Y. Yeshurun, A.P. Malozemoff, and A. Shaulov, Rev. Mod. Phys. **68**, 911 (1996).
[3] A. Gurevich and H. Küpfer, Phys. Rev. B **48**, 6477 (1993).
[4] E.H. Brandt, Phys. Rev. Lett. **76**, 4030 (1996).
[5] E.H. Brandt, Rep. Prog. Phys. **58**, 1465 (1995).
[6] V.M. Vinokur, M.V. Feigel'man, and V. B. Geshkenbein, Phys. Rev. Lett. **67**, 915 (1991).
[7] Y.H. Zhang, H. Luo, X.F. Wu, and S.Y. Ding, Supercond. Sci. Technol. **14**, 346 (2001).
[8] Y.H. Zhang, Z.H. Wang, H. Luo, X.F. Wu, H.M. Luo, Z. Xu, and S.Y. Ding, J. Phys.: Condens. Matter **13**, 2583 (2001).
[9] P. Zhang, C. Ren, S.Y. Ding, Q. Ding, F.Y. Lin, Y.H. Zhang, H. Luo, and X.X. Yao, Supercond. Sci. Technol. **12**, 571 (1999).
[10] L.P. Ma, H.C. Li, R.L. Wang, and L. Li, Physica C **291**, 143 (1997).
[11] Z.Y. Zeng, X.X. Yao, M.J. Qin, Y. Ge, C. Ren, S.Y. Ding, L.P. Ma, H.C. Li, and L. Li, Physica C **291**, 229 (1997).
[12] F. Irie and K. Yamafuji, J. Phys. Soc. Jpn. **23**, 255 (1967).
[13] Only a combination of B_0 and J_{c0} enters the equation. Hence B_0 can be chosen arbitrarily, which will be done below.
[14] For the special case $\alpha=1/(1+\gamma)$, one cannot use Eq. (9); however, we again come to the same Eq. (10) only with an additional factor $K=\mu_0 J_{c0} v_0 \tau/B_0$ at the right-hand side of the equation.
[15] T. Schuster, H. Kuhn, E.H. Brandt, M. Indenbom, M. Koblischka, and M. Konczykowski, Phys. Rev. B **50**, 16 684 (1994).
[16] E.H. Brandt, Phys. Rev. B **55**, 14 513 (1997).
[17] M.E. Gaevski, A.V. Bobyl, D.V. Shantsev, S.F. Karmanenko, Y.M. Galperin, T.H. Johansen, M. Baziljevich, and H. Bratsberg, Phys. Rev. B **59**, 9655 (1999).
[18] D.V. Shantsev, A.V. Bobyl, Y.M. Galperin, and T.H. Johansen, Physica C **341-348**, 1145 (2000).
[19] For the average electric field calculated in Ref. 7 the scaling law is $\int E(x)dx \propto I^{p+\beta}$. For $\alpha=1$, and $\gamma=-1/n$, this exponent equals $1+(n-1)/(n+1)\sim 2$.